RESEARCH ARTICLE

Key Points:
- Active biological ice nuclei are present in the embryos of hailstones
- Water stable isotopes reveal warm, subzero freezing of hailstone embryos
- Layered hailstone growth allows direct study of ice nucleation

Biological ice nucleation initiates hailstone formation

Alexander B. Michaud[1], John E. Dore[1], Deborah Leslie[2], W. Berry Lyons[2], David C. Sands[3], and John C. Priscu[1]

[1]Department of Land Resources and Environmental Sciences, Montana State University, Bozeman, Montana, USA, [2]School of Earth Sciences and Byrd Polar and Climate Research Center, Ohio State University, Columbus, Ohio, USA, [3]Department of Plant Science and Plant Pathology, Montana State University, Bozeman, Montana, USA

Abstract Cloud condensation and ice nuclei in the troposphere are required precursors to cloud and precipitation formation, both of which influence the radiative balance of Earth. The initial stage of hailstone formation (i.e., the embryo) and the subsequent layered growth allow hail to be used as a model for the study of nucleation processes in precipitation. By virtue of the preserved particle and isotopic record captured by hailstones, they represent a unique form of precipitation that allows direct characterization of the particles present during atmospheric ice nucleation. Despite the ecological and economic consequences of hail storms, the dynamics of hailstone nucleation, and thus their formation, are not well understood. Our experiments show that hailstone embryos from three Rocky Mountain storms contained biological ice nuclei capable of freezing water at warm, subzero (°C) temperatures, indicating that biological particles can act as nucleation sites for hailstone formation. These results are corroborated by analysis of δD and $\delta^{18}O$ from melted hailstone embryos, which show that the hailstones formed at similarly warm temperatures in situ. Low densities of ice nucleation active abiotic particles were also present in hailstone embryos, but their low concentration indicates they were not likely to have catalyzed ice formation at the warm temperatures determined from water stable isotope analysis. Our study provides new data on ice nucleation occurring at the bottom of clouds, an atmospheric region whose processes are critical to global climate models but which has challenged instrument-based measurements.

1. Introduction

Atmospheric aerosols play important direct and indirect roles in the radiative balance of Earth. These aerosols directly influence Earth's climate through absorption and reflection of solar radiation in the atmosphere. When these aerosols act as ice nuclei (IN) or cloud condensation nuclei they indirectly affect the climate by forming clouds, which insulate or reflect solar radiation [*Trenberth et al.*, 2007]. Understanding the interactions between aerosol particles and their role in nucleation of tropospheric clouds is critical to developing better global climate models [*Rosenfeld et al.*, 2014].

Convective storms producing large, damaging hail have been a troublesome form of severe weather throughout history [*Changnon and Changnon*, 2000]. Since the early 1800s, many investigators have attempted to explain the causes of hail with the hope of preventing economic losses associated with hailstorms [*Changnon and Ivens*, 1981]. Hailstorms are common in most midlatitude countries, a geographical region hosting large population and agricultural centers [*Leigh and Kuhnel*, 2001; *Changnon et al.*, 2009; *Sioutas et al.*, 2009; *Berthet et al.*, 2011]. In the United States alone, approximately 115,000 hail events occurred between 1996 and 2006 [*National Weather Service*, 2007]. Hail is especially damaging to agriculture because it occurs most frequently during the Northern Hemisphere growing season (May–October) [*Changnon et al.*, 2009]. Thus, hailstone formation has been studied extensively with the goal of prevention. Hail is used in this study to provide data on the processes occurring in the nucleation region of the cloud, a zone which has been challenging to study with instruments [*Rosenfeld et al.*, 2014].

Hailstones are a form of precipitation in which the nucleation event is captured by a distinct unit, the embryo. The embryo is a visually discernable region of a hailstone that typically measures $\approx \leq 5$ mm. Embryos are most commonly (1) frozen-drop embryos, which are produced from the freezing of a raindrop or (2) graupel embryos, which are collections of ice crystals [*Knight and Knight*, 2001]. Newly formed embryos are carried into the main body of a convective storm cloud by warm updrafts [*Knight and Knight*, 2001]. These strong
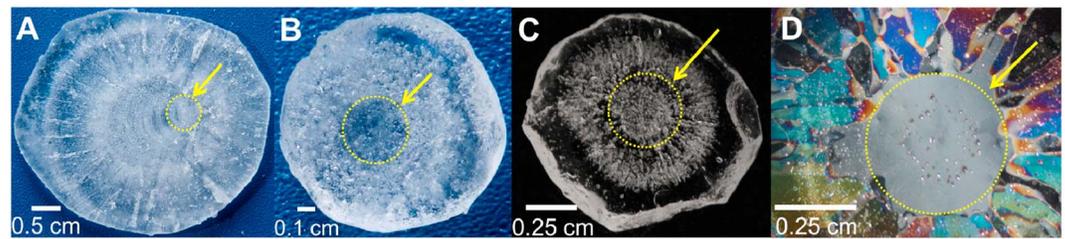
Figure 1. Cross-sectional images of representative hailstones from three Rocky Mountain storms. Yellow arrows and dotted circles denote the embryo. (a–c) Photographs taken under transmitted light and (d) photograph taken under cross-polarized light. Figures 1a–1d represent hailstones from the June 2010, July 2010, August 2011, and July 2010 hailstorms, respectively.

updrafts cycle the hailstone within the storm cloud and allow it to accrete supercooled water. This process produces a layered structure to the hailstone (see Figure 1), which eventually falls to the ground once its weight overcomes the force of the updraft [*Knight and Knight*, 2001]. Thus, hailstone layers are a record of the vertical profile of the storm, and the embryo is a frozen sample of what was present during the nucleation event. This chronological formation of the hailstones' embryo and outer layers overcomes the problem of atmospheric scrubbing that occurs during the descent of rain and snow [*Creamean et al.*, 2013; *Cziczo et al.*, 2013].

Hailstones have been used to track the vertical distributions of chemical and particulate concentrations in storm clouds [*Rosinski*, 1966; *MacGregor et al.*, 1990], while the freezing temperature and trajectory of a hailstone embryo and outer growth layers can be recorded through the use of water stable isotopes (δD- and δ^{18}O-H_2O) [*Jouzel et al.*, 1975, 1985; *Knight et al.*, 1981; *Federer et al.*, 1982]. The relationship between isotopic composition and temperature is based on the decreasing temperature profile with increasing altitude in the troposphere and the equilibrium isotopic fractionation that takes place during condensation. As an air parcel ascends, cools, and condenses in a convective storm cloud, its vapor phase becomes progressively depleted in the heavy isotopologues (δD- and δ^{18}O-H_2O) due to the fact that lower molecular weight isotopologues of water have a higher vapor pressure. Liquid water condensing from this progressively changing air parcel thus also becomes isotopically depleted with increasing altitude and the associated decreasing temperature. During hailstone layer accretion and formation (assuming little or no evaporation takes place), the isotopic signature of the cloud water is preserved and represents an approximate measure of the altitude (and temperature) of layer formation [*Jouzel et al.*, 1985].

An aerosol particle is required for heterogeneous ice nucleation at temperatures associated with lower tropospheric clouds ($> -40°C$) [*Tselioudis et al.*, 1992; *Pruppacher and Klett*, 1998]. Although biological aerosols form a significant fraction of total atmospheric particles, the extent of their role in cloud and ice nucleation remains unclear [*Pöschl et al.*, 2010]. Biological particles (i.e., bacteria, pollen, fungi, and lichens) [see *Hirano and Upper* [1995]; *Després et al.* [2012], and references therein] can be efficient ice nucleators at temperatures $\geq -15°C$. Some abiotic particles are also capable of catalyzing ice nucleation, but their ice nucleation thresholds ($< -15°C$) [*DeMott and Prenni*, 2010] are distinctly colder than those for biological particles; even the most efficient abiotic ice nucleators (e.g., potassium feldspar) require a collectively large surface area or particle number to induce ice nucleation at $> -15°C$ [*Pinti et al.*, 2012; *Atkinson et al.*, 2013]. Our study focused on immersion ice nucleation, which occurs when a particle is immersed in a supercooled water droplet, because it is the dominant freezing process in atmospheric clouds [*Murray et al.*, 2012]. Results from hailstone embryo particle composition and water stable isotopes show that biological IN contribute to hailstone formation.

2. Methods

2.1. Hailstone Collection and Processing

Hailstones were recovered from three northern Rocky Mountain storms near Bozeman, Montana, USA, during the summers of 2010 and 2011. The 30 June 2010 storm produced ~4 cm diameter hailstones, whereas the 21 July 2010 and 29 August 2011 storms produced ~1 cm and ~1.5 cm diameter hailstones,

respectively (Figure 1). Samples were collected in sterile Whirl-Pac bags (Nasco) immediately after they had landed on the ground. Hailstones were transported frozen to our laboratory and were stored at −30°C until processing and analysis.

All hailstones were processed in the SubZero Research Facility at Montana State University, Bozeman, Montana (http://www.coe.montana.edu/ce/subzero/Index.html), in an International Organization for Standardization Class 6 clean cold chamber, operating at −15°C. June 2010 hailstones processed for biological analysis (ice nucleation assay and culturing) were decontaminated according to *Christner et al.* [2005] except for the final melt step. Briefly, the outer layer was scraped with a sterile razor blade, rinsed with 95% ethanol, and followed by a final rinse with sterile deionized water (MilliQ; 18.2 MΩ·cm resistivity). This process removed 13% ± 2.8% of the total hailstone mass. July 2010 and August 2011 hailstones were decontaminated by scraping the outside with a sterile razor blade because the decontamination protocol of *Christner et al.* [2005] eroded too much of each small hailstone. Hailstone layer separation was achieved by slicing the June hail into cross sections using a hot 28 gauge NiChrome wire, in which a 2.4 A current was passed. The surfaces of cross sections were scraped with a sterile razor blade to eliminate interlayer contamination that may have occurred during hot wire cutting. Cross sectioning exposed the hailstone embryo. Embryos from June 2010 cross sections and July 2010 and August 2011 hailstones were isolated using a sterile razor blade. We visually identified and isolated embryos based on the procedures of *Federer et al.* [1982] and *Knight and Knight* [2001]. This isolation was done by first identifying a region of the hailstone that is surrounded by other concentric layers. Depending on the hailstone's trajectory, the embryo can be in the middle or slightly off center. The embryos were ≤5 mm in diameter. Embryos were stored in sterile 50 mL conical tubes at −30°C under further analysis. Samples were allowed to thaw at 4°C for 18 h before analysis.

2.2. Nutrient Analysis

Detection of soluble reactive phosphorus (SRP) in precipitation was used as an indicator of ground-based contamination [*Sheppard*, 2012]. Because phosphorus has no stable gaseous phase, its presence in the atmosphere is almost entirely due to aerosols. SRP concentrations in precipitation are thus low, especially compared to fixed nitrogen species, which have an active atmospheric chemistry. Consequently, a relatively high level of reactive P in precipitation is thus an indicator of ground-based contamination (e.g., from soil organic matter or anthropogenic fertilizer) [see *Sheppard*, 2012]. SRP was determined using the spectrophotometric molybdenum blue assay for SRP [*Murphy and Riley*, 1962] as modified by *Strickland and Parsons* [1968] on melted hailstone embryos. Hailstones from the July storm were cleaned by scraping whole stones as described above. The remaining frozen hailstone material was then melted, and 3 mL of this melt was diluted with MilliQ water up to 10 mL for analysis. Because of the low SRP concentrations expected, a long pathlength (200 cm) liquid waveguide capillary cell (World Precision Instruments) was used in conjunction with a compact spectrometer (Ocean Optics USB4000) for absorbance measurements at 710 nm [*Zhang and Chi*, 2002]. This method as applied had an estimated analytical detection limit of <10 nM SRP.

2.3. Bacterial Culturing and Isolate Collection

R2A (Difco), Nutrient Agar (Difco), and King's B Medium [*King et al.*, 1954] were used to culture heterotrophic, aerobic microorganisms from the embryos of the three hailstorms. These types of media were chosen because R2A is low in nutrients and efficient at culturing stressed organisms which have been frozen in ice [*Christner et al.*, 2001]; nutrient agar is an organic carbon and nutrient rich media, and King's B Medium is a selective media for the known ice nucleation active bacterium, *Pseudomonas syringae* [*King et al.*, 1954]. The plates were inoculated by spread plating 100 μL of hailstone embryo meltwater in quintuplicate. Inoculated plates were enumerated after incubation at room temperature (~21°C) for 3 days. Unique colony morphologies from the three types of media were randomly picked and streaked to isolation. Lyse-n-go (Thermo Scientific) was used to extract genomic DNA to determine the 16S rRNA gene sequence of the isolates. Extracted DNA was amplified using polymerase chain reactions (PCR) in 23 μL volumes and included 11 μL GoTaq 2X Green Master Mix (Promega), 1 μL of 20 μM 9bF primer (5′-AGAGTTTGATCCTGGCTCAG-3′), 1 μL of 20 μM 1492R primer (5′-GGTTACCTTGTTACGACTT-3′) [*Lane*, 1991], 2.5 μL of Lyse-n-go lysate, and 7.5 μL nuclease-free water. The reactions tubes were incubated at 95°C for 10 min, followed by 30 cycles of 95°C for 1 min, 52°C for 30 s, and 72°C for 1 min, and ended with 72°C for 10 min. PCR amplicons were Sanger sequenced (Functional Biosciences) from the 9bF primer and then processed to 500 base pairs, which resulted in high-quality (> 40 Phred score) sequences. The high-quality, trimmed sequences were then

queried against the GenBank database to recover the nearest phylogenetic relative of the isolate. Isolates were named based on the nearest cultured neighbor Basic Local Alignment Search Tool hit. A sequence alignment was performed using ClustalW within the program Molecular Evolutionary Genetics Analysis (MEGA4 v.4.0.2) using the default settings [*Tamura et al.*, 2007]. The evolutionary history of the isolates and the GenBank nearest-neighbor relatives was inferred using the Neighbor-Joining method with bootstrap test of phylogeny (1000 replicates) values displayed at the branch nodes. This phylogenetic analysis was also conducted in MEGA4. The 16S rRNA gene sequences for the hailstone embryo isolates have been deposited in GenBank under accession numbers JX237375–JX237452.

2.4. Ice Nucleation Assay

The ice nucleation assay was based on *Christner et al.* [2008a], with modifications. An aluminum block was machined to fit a 96-well PCR plate and included channels beneath the plate for recirculating a 25% glycol/water coolant solution. The flow-through channels allowed for a consistent temperature (±0.1°C) across the entire plate. Untreated hailstone embryo meltwater (50 μL) from the July 2010 and August 2011 storms was dispensed into each well of a 96-well PCR plate; the June 2010 sample had 93 wells only due to sample volume limitation. The entire plate was cooled through a gradient of temperatures from −2°C to −12°C over a period of 2 h. The number of drops frozen at each 0.5°C interval (IN spectrum) was recorded. After the first IN spectrum was complete, the plate was allowed to thaw at room temperature and then heat treated at 95°C for 10 min [*Christner et al.*, 2008a]. The IN spectrum was determined again after heat treatment to determine the concentration of biological IN. One cumulative IN spectrum and one biological IN spectrum were conducted for each hailstorm. Calculations for total IN and biological IN were based on equation 15 from *Vali* [1971], and modified for the assay volume (50 μL) and degree interval (0.5°C) recorded. The concentration of biological ice nucleators was estimated, at each temperature interval, by measuring the fraction of IN that was inactivated by the heat treatment step.

A modified ice nucleation assay was also used to determine the ice nucleation activity of isolates recovered from the hailstone embryos [*Lindow et al.*, 1978]. Isolates were repeatedly subcultured to ensure purity of the colony. Once a pure colony was obtained, it was transferred to nutrient broth and grown at room temperature. Upon achieving a turbid suspension of the isolate, 500 μL was transferred into 4.5 mL of sterile Phosphate Buffered Saline (PBS) in a 10 mL screw cap test tube. The diluted cultures were incubated at 4°C for 3 h before the assay to allow for the expression of the ice nucleation protein [*Joly et al.*, 2013]. The ice nucleation assay was performed in triplicate for each isolate. These tubes were bathed in a 25% glycol/water solution and cooled from −2°C to −12°C over a period of 2 h. Tubes were visually inspected for frozen contents every 0.5°C. The positive control was *Pseudomonas syringae* strain CC94 (D.C. Sands, Montana State University) [*Morris et al.*, 2007]. Negative controls included sterile PBS and sterile PBS with 500 μL of R2 broth, Nutrient broth, Tryptic Soy Broth, or Luria Broth. The positive control was active between −2.5°C and −3.5°C, while negative controls did not freeze until ≤ −13°C, a typical limit of detection for this assay [*Christner et al.*, 2008a]. An isolate was scored positive for ice nucleation activity if two of the three culture tubes froze before the negative controls in two separate assays.

2.5. Stable Isotope Analysis

Stable isotopes ($\delta^{18}O$ and δD) from a random selection of hailstone embryos from each storm were analyzed with a Picarro Wavelength Scanned-Cavity Ring Down Spectroscopy Analyzer for Isotopic Water Model L1102-*i* and were only thawed immediately before analysis. The stable isotopic analysis includes a calibration using internal laboratory standards of waters spanning the expected isotopic range of the hail samples. The Picarro internal laboratory standards were deionized water aliquots from Colorado, Florida, Ohio, and Nevada, USA. Internal laboratory standards were calibrated relative to Standard Light Antarctic Precipitation and Vienna Standard Mean Ocean Water, at Ohio State Byrd Polar Ice Core Paleoclimatology Laboratory by a duel inlet mass spectrometer. During a Picarro sample run, each thawed sample was pipetted into a 100 μL polyspring glass insert contained in a 2 mL glass sample vial and sealed with a screw cap to prevent evaporation. To eliminate memory effects between samples, six replicate injections of 2 μL were performed, and the results of the first three injections were discarded. Internal laboratory standards were interspersed throughout the run with samples to correct for memory effects. The isotopic results were corrected based on a rolling calibration such that each sample is calibrated by the standards run closest in time to that of the sample. The accuracy was ≤4% for δD and ≤2% for $\delta^{18}O$, calculated by relative standard

error comparing the Picarro isotopic measurement for an internal laboratory standard and the mass spectrometer isotopic measurement for an internal laboratory standard. Precision was ≤1% for δD and ≤0.5% for $\delta^{18}O$, for 100 measurements using relative standard deviation.

We used the stable isotopic composition ($\delta^{18}O$ and δD) of individual hailstone embryos to estimate in situ temperatures of freezing. Although the variation in equilibrium isotopic fractionation of meteoric waters with temperature is predictable and kinetic fractionation in hailstones is typically small [*Federer et al.*, 1982], fixing the temperature scale is problematic, because direct measurements of the isotopic composition of the vapor feeding the clouds are seldom possible. Consequently, we employed two independent empirical approaches to such calibration for our three storms.

Our first approach was to compare isotopic results with those of the similar and well-studied Alberta, Canada, hailstones of August 1971 (Comparison Method) [*Jouzel et al.*, 1975]. The deuterium-temperature relationship for the Alberta hailstones was previously derived from the Isotope Cloud Model (ICM) and the temperature scale fixed using a crystallographic approach [*Jouzel et al.*, 1975, 1985]. Because the strength and duration of hailstorm updrafts differ, the lowest temperature (i.e., highest altitude) at which hailstone layers form is expected to vary considerably between storms. We assumed that following embryo formation, the warmest temperature at which subsequent layers form should represent the base of the main updraft and should be similar between storms producing similar-sized hailstones. Consequently, we assigned the warmest temperature estimated for nonembryo layers of the Alberta hailstones (−14.7°C) to the warmest (highest δD) nonembryo hailstone layer observed during each of the three Montana storms. After fixing the temperature scales of the storms in this way, we used the ICM-based δD-temperature relationship [*Jouzel et al.*, 1975] to infer the temperatures of formation of all other layers, including the embryos.

Our second approach was to take advantage of the interpolated empirically determined climatology of the isotopic composition of precipitation or water isoscape (Isoscapes Method) [*Bowen and Revenaugh*, 2003]. We used the Online Isotopes in Precipitation Calculator (http://www.waterisotopes.org) [*Bowen and Wilkinson*, 2002; *Bowen and Revenaugh*, 2003; *Bowen et al.*, 2005] to generate monthly climatological isotopic values for our Montana location as a function of elevation. We assumed that ground-based precipitation collections represent a mix of waters from the precipitation-forming layers of the clouds above and assigned a particular isotopic value of precipitation to the average temperature of the 1000 m thick layer extending upward from an altitude equivalent to the isoscapes-predicted elevation plus the above-ground height of the cloud base (lower condensation level). To estimate the lower condensation levels for our storms, we utilized radiosonde-collected temperature and dew point data from the nearest NOAA National Weather Service center in Great Falls, Montana. These sonde casts were conducted at local noon on the day of each storm and exhibited typical prethunderstorm structure.

Despite the simplifying assumptions and recognized limitations of all methods that have been used to fix the isotope-temperature scales for hailstones, our two independent approaches yielded similar overall mean (±SD) temperatures for embryo formation in the Montana storms (−14.3 ± 2.7 and −13.5 ± 4.8°C for the comparison and isoscapes approaches, respectively; $n = 14$). In only one case did the predicted embryo formation temperatures differ by more than 3°C. The range of predicted temperatures was narrower for the comparison method than for the isoscapes method (−18.9 to −9.0°C versus −21.8 to −3.1°C, respectively).

2.6. Particle Identification and Analysis

Particles from hailstone embryos were collected via filtration and analyzed with scanning electron microscopy (SEM). Two embryos from the June 2010 storm and five embryos from each of the July 2010 and August 2011 storms were filtered onto a 13 mm, 0.2 μm polytetrafluoroethylene membrane filter (Millipore Corp.) after thawing at 4°C for 18 h. All plasticware used for filtration and sample handling was sterilized and then rinsed 20 times with sterile MilliQ water. Once the particles were filter concentrated, we performed a dehydration step using a graded 0.2 μm filtered ethanol series with two, 5 min incubations at each ethanol step (10, 20, 30, 40, 50, 60, 70, 80, 90, 95, and 100%). The particles were coated before SEM imaging with iridium to a thickness of 5 nm. Images and mineral grain identity were performed on a JEOL JSM-6100 SEM equipped with energy dispersive X-ray spectroscopy (EDX) and a NORAN SiLi detector. Spectrum collection and peak identification were performed using Rontec electronics and software. EDX was performed at 15 kV to obtain spectra of all major elements, and identification of each mineral grain was conducted with a dichotomous key from *Severin* [2004]. The accelerating voltage of 15 kV was sufficient to

identify mineral grains and not too strong to create a large interaction volume and cause filter background effects. Measurement of mineral grain size was done using the program ImageJ [*Abrámoff et al.*, 2004]. Large biological particles were visually identified (L. Szabo and Y. Jin, personal communication, 2012).

Procedural controls were prepared and analyzed in parallel with the hailstone samples. Small cubes of MilliQ water were frozen and then cleaned with the same technique as the hailstones. These cleaned MilliQ ice cubes were filtered and subjected to the same ethanol dehydration series. Particles on the control filter were imaged and identified with the same SEM-EDX methodology. The total number of particles and composition was insignificant compared to the particles found on the embryo samples. An elemental spectrum was collected from the control filter as a reference for its composition.

Statistical tests comparing freezing temperatures of embryo derived particles, stable isotope derived temperatures, and those data reviewed from other studies were conducted using SigmaPlot v11.0. One-way analysis of variance (ANOVA) was applied between treatment groups, and data passed normality and equal variance tests. Pairwise comparisons were conducted with the Holm-Sidak method. Comparison of the two isotope temperature methods, comparative and isoscapes, was conducted using a two-sided t test.

## 3. Results and Discussion

3.1. Ground-Based Contamination

We used SRP as an indicator of ground-based contamination in hailstone embryo meltwater. The concentration of SRP in July hailstone embryos was below the limit of detection (<10 nM), demonstrating that our decontamination procedures successfully removed any material that the hailstones may have acquired from soils or vegetation after falling on the ground.

3.2. Embryo Freezing Temperatures

Stable isotopes (δD and $\delta^{18}O$) of hailstone embryo meltwater were measured to determine the in situ temperature of embryo formation. The average in situ embryo formation temperatures from the June 2010, July 2010, and August 2011 storms derived from the stable isotope comparative method were -13.1, -16.5, and $-11.4°C$, whereas those derived from the isoscapes method were -11.4, -16.9, and $-9.1°C$ (Figure 2). The overall means ($\pm SD$) for the two methods were $-13.5°C$ (± 4.8) and $-14.3°C$ (± 2.7), respectively, which are not statistically different ($t = 0.547$; df $= 26$; $P > 0.5$). The overall mean embryo freezing temperatures are warmer than typical abiotic ice nucleation temperatures ($< -15°C$) [*DeMott and Prenni*, 2010] and not significantly different (one-way ANOVA, $P = 0.273$) from the results of other stable isotope studies that investigated the temperatures of embryo freezing and hailstone growth [*Knight et al.*, 1981; *Jouzel et al.*, 1985] (Figure 2). The July 2010 hailstorm embryos formed at a significantly colder temperature than those from the other two storms. Their formation could have been catalyzed by biological ice nuclei or by the most efficient of the abiotic ice nuclei (e.g., K-feldspars). Alternatively, the colder apparent formation temperatures of these relatively small hailstones may result from contamination of the embryos with ice from the innermost growth layers during the difficult embryo isolation process. Most ($>91\%$) of the hailstones examined in earlier studies showed that embryos formed at temperatures $> -14°C$, but no mechanisms were proposed to explain hailstone embryos freezing at these warm temperatures [*Knight et al.*, 1981]. δD and $\delta^{18}O$ data from hailstone embryos in our study corroborate results from studies of embryo freezing temperatures and correspond to the freezing temperatures of other known biological ice nuclei (Figure 2). The relatively warm freezing temperatures determined from stable isotopes in our study and in previous studies reveal that only the most efficient ice nucleators (e.g., biological ice nuclei) likely initiate hailstone embryo formation.
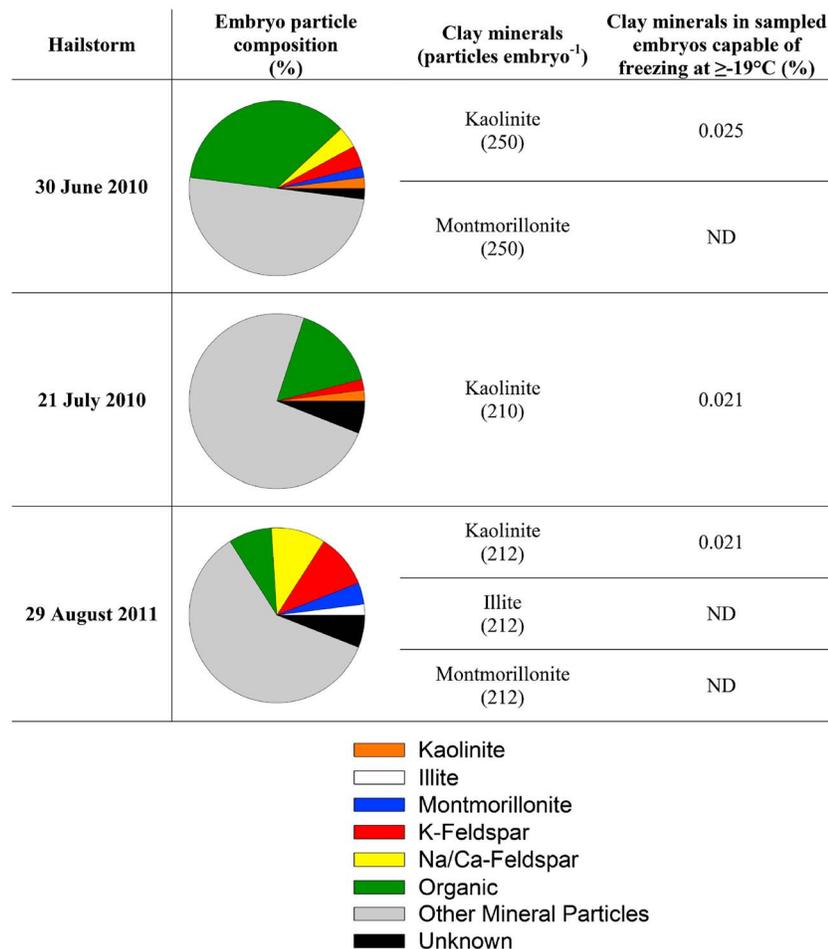
3.3. Biologically Mediated Ice Nucleation

Ice nucleation active biological particles are characteristically active from $-2°C$ to $-18°C$ with the majority of biologically mediated nucleation occurring at temperatures $> -15°C$ (Figure 2) [*Hirano and Upper*, 1995; *Després et al.*, 2012]. Our experimental results show that biological ice nuclei from hailstone embryos began to nucleate ice at temperatures of $-5°C$, $-7.5°C$, and $-7°C$ for the June 2010, July 2010, and August 2011 storms, respectively (Figure 2; see "Biological Ice Nuclei"). The estimated concentrations of biological ice nuclei measured at these temperatures were 3, 6, and 8 biological ice nuclei per mL of embryo meltwater, respectively. These concentrations are equivalent to ~1 biological ice nucleus embryo^{-1} and
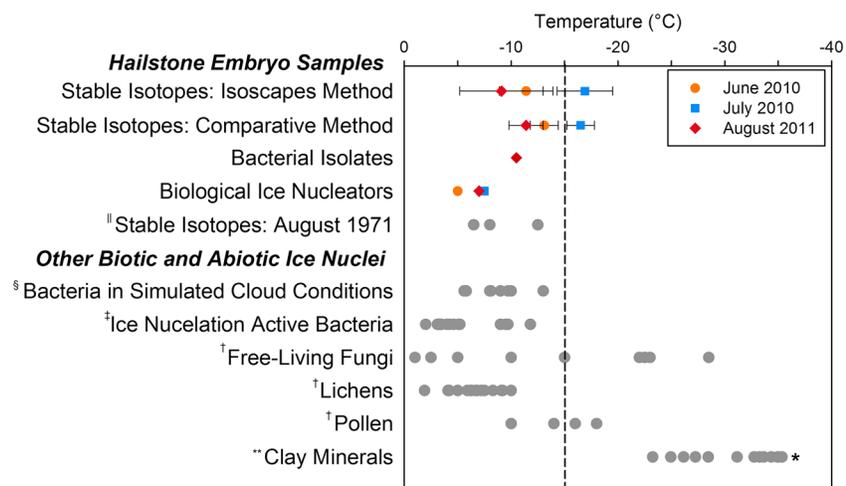
Figure 2. Freezing point temperatures computed from four different methods for embryos from hailstorms occurring in the Rocky Mountain region on 30 June 2010 (orange circles), 21 July 2010 (blue squares), and 29 August 2011 (crimson diamonds). The dashed vertical line represents the warmest abiotic nucleation temperature reported by *DeMott and Prenni* [2010]. The single asterisk within the panel indicates that the temperature of nucleation for abiotic particles is significantly different (*P* < 0.001) from biological ice nucleation temperatures and isotopically determined freezing temperatures presented. The right side of the figure is bounded by the warmest temperature at which water will homogenously freeze without a biotic or abiotic ice nucleator at −40°C [*Pruppacher and Klett*, 1998]. Double vertical line denotes data from *Jouzel et al.* [1985]; section sign denotes data from *Möhler et al.* [2007]; double dagger denotes data from *Hirano and Upper* [1995], *Després et al.* [2012], and citations therein; dagger denotes data from *Diehl et al.* [2001], *Diehl et al.* [2002], *Després et al.* [2012] and citation therein; and two asterisks denote data from *Pinti et al.* [2012].

are approximately 10 times higher than reported values for rain at comparable temperatures [*Christner et al.*, 2008a], revealing a relatively high in situ concentration of biological ice nuclei active at warm temperatures in hailstone embryos. Further evidence for abundant biological ice nucleation in hail was found by *Hill et al.* [2014] who used quantitative PCR to determine the number of *ina* gene copies present in hailstones; this gene codes for the proteins responsible for biological ice nucleation activity at relatively warm temperatures (up to −2°C). The comparatively high *ina* gene copy number in hailstones was concluded by *Hill et al.* [2014] to indicate a significant source of warm ice nucleating particles. Particulate matter analysis showed that organic particles constituted between 8 and 34% of the total particles in these samples (Figure 3 and Figures S1 and S2 in the supporting information). Visual identification of particles categorized as organic showed that these particles were composed of fungal spores, pollen grains, and other organic detritus. Fungal urediospores were common biological particles in hailstone embryos (Figure S2 in the supporting information). *Morris et al.* [2013] showed that these spores are ice nucleation active and possess ice nucleating species of bacteria on their surface. These spores may have contributed to nucleation of the hailstones we studied. Rain and snow have also been shown to contain biological particles that are ice nucleation active at warm, subzero temperatures [*Christner et al.*, 2008a, 2008b]. However, rain and snow can scavenge other ice nucleating material during their descent [*Creamean et al.*, 2013; *Cziczo et al.*, 2013], producing a ground-based sample that may not be representative of the particles present in the nucleation region of the cloud. Atmospheric scavenging precludes detailed study of the processes initiating nucleation and leaves the role of biological ice nucleation in rain and snow equivocal. The distinct embryo phase of hailstones preserves the composition of ice nuclei responsible for warm, subzero embryo nucleation and spatially segregates the embryos from outer hailstone growth layers [*Knight and Knight*, 2001].

Bacterial cultures from melted embryos yielded 12–535 colony forming units (CFU) embryo^{-1}. The assemblage of bacteria we isolated from hailstone embryos contained similar types of bacteria to those previously recovered from hailstones [*Harrison*, 1898; *Mandrioli et al.*, 1973; *Temkiv et al.*, 2012; *Šantl-Temkiv et al.*, 2013]. A subset (50; 2% of all CFU; *n* = 2448) (Figure S3 in the supporting information) was tested for the ability to nucleate ice. Within the subset of bacteria tested, we isolated one ice nucleation active organism related (>97% rRNA gene sequence similarity) to *Pantoea stewartii* (syn. *Erwinia stewartii*), a

Hailstorm	Embryo particle composition (%)	Clay minerals (particles embryo^{-1})	Clay minerals in sampled embryos capable of freezing at ≥-19°C (%)
30 June 2010		Kaolinite (250)	0.025
		Montmorillonite (250)	ND
21 July 2010		Kaolinite (210)	0.021
29 August 2011		Kaolinite (212)	0.021
		Illite (212)	ND
		Montmorillonite (212)	ND

Legend:
- 🟧 Kaolinite
- ⬜ Illite
- 🟦 Montmorillonite
- 🟥 K-Feldspar
- 🟨 Na/Ca-Feldspar
- 🟩 Organic
- ⬜ Other Mineral Particles
- ⬛ Unknown

Figure 3. Particle composition found in hailstone embryos from three Rocky Mountain storms. Diagrams represent percent of particles analyzed by SEM-EDX within each embryo (n = 50). The density of clay minerals per embryo was estimated by multiplying total particles within the embryo by the percent composition shown in the pie diagrams. The percentage of kaolinite particles capable of freezing at warmer than −19°C for each storm was determined by multiplying the density of kaolinite particles within each embryo by the fraction (0.0001%) of particles shown to be active at ≥ −19°C by *Pinti et al.* [2012]. ND = the percentage of ice nucleation active particles was not determined by *Pinti et al.* [2012] for these clay minerals.

known ice nucleation active organism [*Wallin et al.*, 1979; *Mergaert et al.*, 1993]. Our isolate possessed a freezing temperature of −10.5°C in our nucleation experiments (Figure 2), which is colder than the maximum nucleation temperature for *Pseudomonas syringae* (−2°C) [*Morris et al.*, 2014], but is similar to the in situ freezing point that we determined for embryos using stable isotopes of water (Figure 2). Because we only tested 2% of all the CFUs obtained during culturing of hailstone embryo meltwater, it is possible that more ice nucleation active isolates were present in the hailstones samples. The number of colony forming units obtained by our culturing efforts (519 CFU mL^{-1}) is similar to the high end of the range reported by *Šantl-Temkiv et al.* [2013] (20–500 CFU mL^{-1}) who studied meltwater from whole hailstones (embryos and outer layers) collected from a storm in Europe. Our examination of the small subunit ribosomal RNA gene sequences deposited in GenBank by *Šantl-Temkiv et al.* [2013] showed that the ice nucleation active bacterium (>98.5% 16S rRNA gene sequence similarity) *Pseudomonas fluorescens* represented 1.8% of all sequences they recovered from hailstones. Molecular evidence of ice nucleation active bacteria shows the potential for these bacteria to be active in nucleating hailstones, yet only a fraction of these bacteria may exhibit the ice nucleation phenotype. Our results reveal that ice nucleation active bacteria, albeit in low abundance, are present in hailstone embryos.
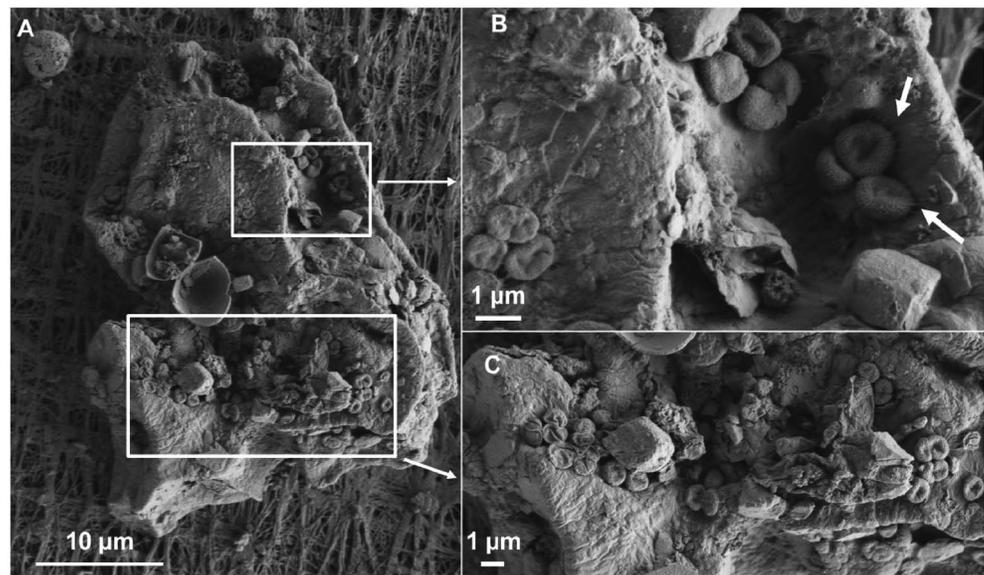
Figure 4. (a) A montmorillonite clay mineral particle from a 29 August 2011 embryo showing biological material on the surface. (b) Magnification of white box in Figure 4a. Arrows in Figure 4b reveal the close association between the mineral grain and biological particles, and show filamentous structures which attach the biological particles to the mineral surface. (c) Magnification of white box in Figure 4a showing the diversity of cell morphologies present on the clay grain surface.

3.4. Abiotic Ice Nucleation

Abiotic particles have recently been shown to be a component of total ice nuclei in clouds [*Atkinson et al.*, 2013; *Cziczo et al.*, 2013]. To explore the possibility of abiotic ice nucleation in hailstone embryos, we determined whether known abiotic ice nucleation active particles were present. Total (biotic + abiotic) particle concentrations in the hailstones we studied were 1.24×10^4, 1.04×10^4, and 1.05×10^4 particles ($\geq 1.5\ \mu m$) embryo^{-1} for hailstones collected from the June 2010, July 2010, and August 2011 storms, respectively. These particle concentrations are similar to insoluble particle concentrations detected in the embryo region of the hailstones studied by *Rosinski and Kerrigan* [1969]. Talc and biotite, which are not known to be significant immersion ice nucleators [*Murray et al.*, 2012], were the most abundant abiotic particles in our study, collectively compromising 16 to 48% of the total particles contained within the embryos of the three storms (Figure 3 and Figure S1 in the supporting information). The sum of the three well-studied ice nucleation active clays illite, kaolinite, and montmorillonite [*Pinti et al.*, 2012] constituted only 2 to 6% of the particles sampled from embryos in our study (Figure 3). Only 0.0001% of kaolinite particles possess an ideal nucleation site and are ice nucleation active at temperatures warmer than $-19°C$ [*Pinti et al.*, 2012]. Therefore, the embryos sampled in our study would require a >4000-fold increase in kaolinite particles to achieve densities likely to produce an ice nucleus at temperatures $\geq -19°C$. These three clay types have long been considered the most efficient abiotic ice nuclei in the atmosphere [*Pruppacher and Klett*, 1998], but their ice nucleation activity is likely due to their overwhelming concentration in the atmosphere, especially during dust storms [*Pinti et al.*, 2012], rather than to their high-specific nucleation activity. The relatively low abundance of illite, kaolinite, and montmorillonite in our hailstone embryos indicates that these abiotic particles are unlikely to have initiated nucleation of the embryos in the hailstones we analyzed (Figure 3).

Atkinson et al. [2013] contended that potassium feldspar (K-feldspar) minerals are highly ice nucleation active, supporting a report that potassium-rich mica possesses warm ice nucleation activity [*Shen et al.*, 1977]. Atkinson and colleagues further argued that K-feldspar is a more efficient ice nucleator than clay minerals, in contrast to other studies showing that clay minerals are the most efficient abiotic ice nuclei [*Pruppacher and Klett*, 1998; *Pinti et al.*, 2012]. K-feldspar was a minor component of the particle analysis in the embryos we studied, constituting 2 to 10% of the total particles. August embryo samples had the highest concentration of K-feldspar. We used the average size of measured K-feldspar particles to calculate a

total spherical equivalent surface area and concluded that the August embryos would need a 159-fold increase in surface area to have $1\,cm^2$ and possess 1 active nucleation site at $-8°C$ [*Atkinson et al.*, 2013]. Despite the August storm having the best chance of K-feldspar nucleation, the stable isotope analysis showed these embryos froze within the temperature of freezing range of the biological ice nuclei reported in Figure 2. Although some abiotic particles are potentially ice nucleation active, they require a relatively higher concentration of particles in order to catalyze ice formation when compared to biological particles at the same temperature [*Després et al.*, 2012]. The dependence of high abiotic particle concentration on warm ice nucleation is because of their relatively low ice nucleating fraction [*Després et al.*, 2012]; this dependence on high surface area is applicable to specific clays and K-feldspar particles alike [*Atkinson et al.*, 2013].

Although abiotic particles can contribute to atmospheric ice nucleation, their contribution may be more commonly as a substrate for attachment of ice nucleating bacteria or biological particles rather than as direct nucleation sites [*Conen et al.*, 2011]. Our electron microscopic observations revealed that biological particles were attached to abiotic particles in hailstone embryos (Figure 4 and Figure S2 in the supporting information) and may have been the primary nucleation agents. The results of *Creamean et al.* [2013] support this contention, as they found >50% of precipitation residues contained biological material and dust. Others [*Zimmermann et al.*, 2008; *Ariya et al.*, 2009] have reported anomalously warm ($> -19°C$) ice nucleation temperatures for mineral particles but did not consider the possibility that attached bacteria or other biological ice nuclei could have been present on their surfaces.

4. Conclusions

The chronological structure of ice layers within hailstones provides a model system that allows direct study of the connection between biological ice nucleation, temperatures of nucleation, and the formation of precipitation. The present lack of instrumentation to measure cloud bottom properties and specific aerosols directly has led to a paucity of high-quality data to use in models of cloud dynamics, which are ultimately incorporated into global climate simulations. The major challenge of modeling aerosol effects on cloud properties centers on the nucleation region of the cloud [*Rosenfeld et al.*, 2014]. Specifically, our data reveal that biological particles are abundant within hailstone embryos and are active at warm temperatures; hence, they are critically important ice nuclei within the nucleation region of storm clouds.

Author Contributions

A.B.M. designed research; A.B.M. performed research; D.L., W.B.L., J.E.D., and A.B.M. performed stable isotope analysis; A.B.M., J.E.D., J.C.P., and D.C.S. analyzed data; A.B.M., J.E.D., and J.C.P. wrote the paper; all authors approved the final draft.

References

Abrámoff, M. D., P. J. Magalhães, and S. J. Ram (2004), Image processing with ImageJ, *Biophotonics Int.*, *11*(7), 36–42.

Ariya, P. A., J. Sun, N. A. Eltouny, E. D. Hudson, C. T. Hayes, and G. Kos (2009), Physical and chemical characterization of bioaerosols— Implications for nucleation processes, *Int. Rev. Phys. Chem.*, *28*(1), 1–32, doi:10.1080/01442350802597438.

Atkinson, J. D., B. J. Murray, M. T. Woodhouse, T. F. Whale, K. J. Baustian, K. S. Carslaw, S. Dobbie, D. O'Sullivan, and T. L. Malkin (2013), The importance of feldspar for ice nucleation by mineral dust in mixed-phase clouds, *Nature*, *498*, 355–358, doi:10.1038/nature12278.

Berthet, C., J. Dessens, and J. L. Sanchez (2011), Regional and yearly variations of hail frequency and intensity in France, *Atmos. Res.*, *100*(4), 391–400, doi:10.1016/j.atmosres.2010.10.008.

Bowen, G. J., and J. Revenaugh (2003), Interpolating the isotopic composition of modern meteoric precipitation, *Water Resour. Res.*, *39*(10), 1299, doi:10.1029/2003WR002086.

Bowen, G. J., and B. Wilkinson (2002), Spatial distribution of $\delta^{18}O$ in meteoric precipitation, *Geology*, *30*(4), 315–318.

Bowen, G. J., L. I. Wassenaar, and K. A. Hobson (2005), Global application of stable hydrogen and oxygen isotopes to wildlife forensics, *Oecologia*, *143*(3), 337–348, doi:10.1007/s00442-004-1813-y.

Changnon, S. A., and D. Changnon (2000), Long-term fluctuations in hail incidences in the United States, *J. Clim.*, *13*(3), 658–665.

Changnon, S. A., and J. L. Ivens (1981), History repeated: The forgotten hail cannons of Europe, *Am. Meterol. Soc.*, *62*(3), 368–375.

Changnon, S. A., D. Changnon, and S. D. Hilberg (2009), *Hailstorms Across the Nation: An Atlas About Hail and Its Damages*, Illinois State Water Survey A division of the Institute of Natural Resource Sustainability, Champaign, Ill.

Christner, B. C., E. Mosley-Thompson, L. G. Thompson, and J. N. Reeve (2001), Isolation of bacteria and 16S rDNAs from Lake Vostok accretion ice, *Environ. Microbiol.*, *3*(9), 570–577.

Christner, B. C., J. A. Mikucki, C. M. Foreman, J. Denson, and J. C. Priscu (2005), Glacial ice cores: A model system for developing extraterrestrial decontamination protocols, *Icarus*, *174*(2), 572–584.

Christner, B. C., R. Cai, C. E. Morris, K. S. McCarter, C. M. Foreman, M. L. Skidmore, S. N. Montross, and D. C. Sands (2008a), Geographic, seasonal, and precipitation chemistry influence on the abundance and activity of biological ice nucleators in rain and snow, *Proc. Natl. Acad. Sci. U.S.A.*, *105*(48), 18,854–18,859, doi:10.1073/pnas.0809816105.

Christner, B. C., C. E. Morris, C. M. Foreman, R. Cai, and D. C. Sands (2008b), Ubiquity of biological ice nucleators in snowfall, *Science*, *319*(5867), 1214, doi:10.1126/science.1149757.

Conen, F., C. E. Morris, J. Leifeld, M. V. Yakutin, and C. Alewell (2011), Biological residues define the ice nucleation properties of soil dust, *Atmos. Chem. Phys.*, *11*(18), 9643–9648, doi:10.5194/acp-11-9643-2011.

Creamean, J. M., et al. (2013), Dust and biological aerosols from the Sahara and Asia influence precipitation in the western U.S., *Science*, *1572*, 1572–1578.

Cziczo, D. J., K. D. Froyd, C. Hoose, E. J. Jensen, M. Diao, M. A. Zondlo, J. B. Smith, C. H. Twohy, and D. M. Murphy (2013), Clarifying the dominant sources and mechanisms of cirrus cloud formation, *Science*, *340*, 1320–1324, doi:10.1126/science.1234145.

DeMott, P. J., and A. J. Prenni (2010), New directions: Need for defining the numbers and sources of biological aerosols acting as ice nuclei, *Atmos. Environ.*, *44*(15), 1944–1945.

Després, V. R., et al. (2012), Primary biological aerosol particles in the atmosphere: A review, *Tellus B*, *64*, doi:10.3402/tellusb.v64i0.15598.

Diehl, K., C. Quick, S. Matthias-Maser, and S. K. Mitra (2001), The ice nucleating ability of pollen Part I: Laboratory studies in deposition and condensation freezing modes, *Atmos. Res.*, *58*(2), 75–87.

Diehl, K., S. Matthians-Maser, R. Jenicke, and S. K. Mitra (2002), The ice nucleating ability of pollen: Part II. Laboratory studies in immersion and contact freezing modes, *Atmos. Res.*, *61*(2), 125–133, doi:10.S0169-8095(01)00132-6.

Federer, B., N. Brichet, and J. Jouzel (1982), Stable isotopes in hailstones. Part I: The isotopic cloud model, *Am. Meterol. Soc.*, *39*, 1323–1335.

Harrison, F. C. (1898), Bacterial content of hailstones, *Bot. Gaz.*, *26*(3), 211–214.

Hill, T. C. J., B. F. Moffett, P. J. DeMott, D. G. Georgakopoulos, W. L. Stump, and G. D. Franc (2014), Measurement of ice nucleation-active bacteria on plants and in precipitation by quantitative PCR, *Appl. Environ. Microbiol.*, *80*(4), 1256–67, doi:10.1128/AEM.02967-13.

Hirano, S. S., and C. D. Upper (1995), Ecology of ice nucleation-active bacteria, in *Biological Ice Nucleation and Its Applications*, edited by R. E. Lee, G. J. Warren, and L. V. Gusta, pp. 370, The American Phytopathological Society, St. Paul, Minn.

Joly, M., E. Attard, M. Sancelme, L. Deguillaume, C. Guilbaud, C. E. Morris, P. Amato, and A.-M. Delort (2013), Ice nucleation activity of bacteria isolated from cloud water, *Atmos. Environ.*, *70*, 392–400, doi:10.1016/j.atmosenv.2013.01.027.

Jouzel, J., L. Merlivat, and E. Roth (1975), Isotopic study of hail, *J. Geophys. Res.*, *80*(36), 5015–5030, doi:10.1029/JC080i036p05015.

Jouzel, J., L. Merlivat, and B. Federer (1985), Isotopic study of hail: The δD-$\delta^{18}O$ relationship and the growth history of large hailstones, *Q. J. R. Meteorol. Soc.*, *111*, 495–516.

King, E. O., M. K. Ward, and D. E. Raney (1954), Two simple media for the demonstration of pyocyanin and fluorescein, *J. Lab. Clin. Med.*, *44*, 301–307.

Knight, C. A., and N. C. Knight (2001), Hailstorms, in *Severe Convective Storms*, edited by C. A. Doswell, pp. 570, Am. Meteorol. Soc., Boston, Mass.

Knight, C. A., N. C. Knight, and K. A. Kime (1981), Deuterium contents of storm inflow and hailstone growth layers, *J. Atmos. Sci.*, *38*(11), 2485–2499.

Lane, D. J. (1991), 16S/23S rRNA sequencing, in *Nucleic Acid Techniques in Bacterial Systematics*, edited by E. Stackebrandt and M. Goodfellow, pp. 115–175, John Wiley, New York.

Leigh, R., and I. Kuhnel (2001), Hailstorm loss modelling and risk assessment in the Sydney region, Australia, *Nat. Hazards*, *24*, 171–185.

Lindow, S. E., D. C. Arny, and C. D. Upper (1978), *Erwinia herbicola*: A bacterial ice nucleus active in increasing frost injury to corn, *Phytopathology*, *68*(3), 523–527, doi:10.1094/Phyto-68-523.

MacGregor, L., H. G. Marshall, N. C. Knight, C. A. Knight, J. C. Farmer, and H. Westberg (1990), Hailstones as cloud water composition probes: An initial assessment, *Atmos. Environ.*, *24*(8), 2247–2251, doi:10.1016/0960-1686(90)90256-M.

Mandrioli, P., G. L. Puppi, N. Bagni, and F. Prodi (1973), Distribution of microorganisms in hailstones, *Nature*, *246*(5433), 416–417.

Mergaert, J., L. Verdonck, and K. Kersters (1993), Transfer of *Erwinia ananas* (synonym, *Erwinia uredovora*) and *Erwinia stewartii* to the genus *Pantoea* emend. as *Pantoea ananas* (Serrano 1928) comb. nov. and *Pantoea stewartii* (Smith 1898) comb. nov., respectively, and description of *Pantoea stewartii* subsp. *indologenes* subs. nov, *Int. J. Syst. Bacteriol.*, *43*(1), 162–173.

Möhler, O., P. J. DeMott, G. Vali, and Z. Levin (2007), Microbiology and atmospheric processes: The role of biological particles in cloud physics, *Biogeosciences*, *4*(6), 1059–1071, doi:10.5194/bg-4-1059-2007.

Morris, C. E., L. L. Kinkel, K. Xiao, P. Prior, and D. C. Sands (2007), Surprising niche for the plant pathogen *Pseudomonas syringae*, *Infect. Genet. Evol.*, *7*(1), 84–92.

Morris, C. E., D. C. Sands, C. Glaux, J. Samsatly, S. Asaad, A. R. Moukahel, F. L. T. Gonçalves, and E. K. Bigg (2013), Urediospores of rust fungi are ice nucleation active at > −10°C and harbor ice nucleation active bacteria, *Atmos. Chem. Phys.*, *13*(8), 4223–4233, doi:10.5194/acp-13-4223-2013.

Morris, C. E., F. Conen, J. A. Huffman, V. Phillips, U. Pöschl, and D. C. Sands (2014), Bioprecipitation: A feedback cycle linking Earth history, ecosystem dynamics and land use through biological ice nucleators in the atmosphere, *Global Change Biol.*, *20*(2), 341–51, doi:10.1111/gcb.12447.

Murphy, J., and J. P. Riley (1962), A modified single solution method for the determination of phosphate in natural waters, *Anal. Chim. Acta*, *27*, 31–36.

Murray, B. J., D. O'Sullivan, J. D. Atkinson, and M. E. Webb (2012), Ice nucleation by particles immersed in supercooled cloud droplets, *Chem. Soc. Rev.*, *41*(19), 6519–6554, doi:10.1039/c2cs35200a.

National Weather Service (2007), Storm Data Database, Natl. Clim. Data Cent., National Oceanic and Atmospheric Administration. [Available at http://www.ncdc.noaa.gov/stormevents/.]

Pinti, V., C. Marcolli, B. Zobrist, C. R. Hoyle, and T. Peter (2012), Ice nucleation efficiency of clay minerals in the immersion mode, *Atmos. Chem. Phys. Discuss.*, *12*(1), 3213–3261, doi:10.5194/acpd-12-3213-2012.

Pöschl, U., et al. (2010), Rainforest aerosols as biogenic nuclei of clouds and precipitation in the Amazon, *Science*, *329*(5998), 1513–1516, doi:10.1126/science.1191056.

Pruppacher, H. R., and J. D. Klett (1998), *Microphysics of Clouds and Precipitation*, 2nd ed., Springer, New York.

Rosenfeld, D., S. Sherwood, R. Wood, and L. Donner (2014), Climate effects of aerosol-cloud interactions, *Science*, *343*(6169), 379–380, doi:10.1126/science.1247490.

Rosinski, J. (1966), Solid water-insoluble particles in hailstones and their geophysical significance, *J. Appl. Meteorol.*, *5*, 481–492.

Rosinski, J., and T. C. Kerrigan (1969), The role of aerosol particles in the formation of raindrops and hailstones in severe thunderstorms, *J. Atmos. Sci.*, *26*, 695–715.

Šantl-Temkiv, T., K. Finster, T. Dittmar, B. M. Hansen, R. Thyrhaug, N. W. Nielsen, and U. G. Karlson (2013), Hailstones: A window into the microbial and chemical inventory of a storm cloud., *PLoS One*, *8*(1), e53550, doi: 10.1371/journal.pone.0053550.

Severin, K. P. (2004), *Energy Dispersive Spectrometry of Common Rock Forming Minerals*, Kluwer Acad., Boston, Mass.

Shen, J. H., K. Klier, and C. A. Zettlemoyer (1977), Ice nucleation by micas, *J. Atmos. Sci.*, *34*, 957–960.

Sheppard, L. (2012), National Atmospheric Deposition Program 2011 Annual Summary. [Available at http://nadp.sws.uiuc.edu/lib/data/2011as.pdf.]

Sioutas, M., T. Meaden, and J. D. C. Webb (2009), Hail frequency, distribution and intensity in Northern Greece, *Atmos. Res.*, *93*(1–3), 526–533, doi:10.1016/j.atmosres.2008.09.023.

Strickland, J. D. H., and T. R. Parsons (1968), *A Practical Handbook of Seawater Analysis*, Fisheries Research Board of Canada, Ottawa.

Tamura, K., J. Dudley, M. Nei, and S. Kumar (2007), MEGA 4: Molecular Evolutionary Genetics Analysis (MEGA) software version 4.0, *Mol. Biol. Evol.*, *24*, 1596–1599.

Temkiv, T. Š., K. Finster, B. M. Hansen, N. W. Nielsen, and U. G. Karlson (2012), The microbial diversity of a storm cloud as assessed by hailstones, *FEMS Microbiol. Ecol.*, *81*(3), 684–695.

Trenberth, K. E., et al. (2007), Observations: Surface and atmospheric climate change, in *Climate Change 2007: The Physical Science Basis. Contribution of Working Group I to the Fourth Assessment Report of the Intergovernmental Panel on Climate Change*, edited by S. Solomon et al., pp. 996, Cambridge Univ. Press, Cambridge, U. K.

Tselioudis, G., W. B. Rossow, and D. Rind (1992), Global patterns of cloud optical thickness variation with temperature, *J. Clim.*, *5*, 1484–1495.

Vali, G. (1971), Quantitative evaluation of experimental results on the heterogeneous freezing nucleation of supercooled liquids, *J. Atmos. Sci.*, *28*, 402–409.

Wallin, J. R., D. V. Loonan, and C. A. C. Gardner (1979), *Erwinia stewartii*: An ice nucleus for frost damage to maize seedlings, *Plant Dis. Rep.*, *63*, 751–752.

Zhang, J.-Z., and J. Chi (2002), Automated analysis of nanomolar concentrations of phosphate in natural water with liquid waveguide, *Environ. Sci. Technol.*, *36*, 1048–1053.

Zimmermann, F., S. Weinbruch, L. Schütz, H. Hofmann, M. Ebert, K. Kandler, and A. Worringen (2008), Ice nucleation properties of the most abundant mineral dust phases, *J. Geophys. Res.*, *113*, D23204, doi:10.1029/2008JD010655.